Published in final edited form as:
Dev Dyn. 2008 July ; 237(7): 1780–1788. doi:10.1002/dvdy.21581.

The Zebrafish Embryo as a Dynamic Model of Anoxia Tolerance

Bryce A. Mendelsohn, **Bethany L. Kassebaum**, and **Jonathan D. Gitlin***
Edward Mallinckrodt Department of Pediatrics Washington University School of Medicine St. Louis, Missouri 63110, USA

Abstract

Developing organisms depend upon a delicate balance in the supply and demand of energy to adapt to variable oxygen availability, though the essential mechanisms determining such adaptation remain elusive. In this study we examine reversible anoxic arrest and dynamic bioenergetic transitions during zebrafish development. Our data reveal that the duration of anoxic viability corresponds to the developmental stage and anaerobic metabolic rate. Diverse chemical inhibitors of mitochondrial oxidative phosphorylation induce a similar arrest in normoxic embryos, suggesting a pathway responsive to perturbations in aerobic energy production rather than molecular oxygen. Consistent with this concept, arrest is accompanied by rapid activation of the energy-sensing AMP-activated protein kinase pathway, demonstrating a potential link between the sensing of energy status and adaptation to oxygen availability. These observations permit mechanistic insight into energy homeostasis during development that now enable genetic and small molecule screens in this vertebrate model of anoxia tolerance.

Keywords

zebrafish; mitochondria; AMPK; growth control

Introduction

Teleost embryos require oxygen for development, and as this vital nutrient is not supplied by the yolk, mechanisms have evolved to permit adaptation to variable environmental oxygen availability. These adaptations are essential to maintain intracellular energy homeostasis as well as to synchronize intercellular processes such as patterning, motility and differentiation. The developmental responses to perturbations in energy production thus form a fundamental regulatory component of embryogenesis. The capacity of some species to adapt to limited oxygen is extreme, and studies in teleost embryos have described a complete, prolonged, yet reversible developmental arrest in response to anoxia or some chemical inhibitors of oxidative phosphorylation (Crawford and Wilde, 1966; Padilla and Roth, 2001; Podrabsky et al., 2007). Nevertheless, the mechanisms by which anoxia is sensed and the subsequent processes permitting arrest and recovery remain largely unknown (Guppy and Withers, 1999; Kemp, 2006).

At the same time, significant progress has been achieved in defining the complex molecular activities of several oxygen- and energy-sensing pathways including the hypoxia inducible factor (HIF) and the AMP-activated protein kinase (AMPK) pathways, which have been implicated in diverse yet fundamental processes such as angiogenesis, tumorigenesis, and

*Corresponding Author: Jonathan D. Gitlin, M.D. Edward Mallinckrodt Department of Pediatrics Washington University School of Medicine 660 South Euclid Avenue, Box 8208 St. Louis, Missouri 63110 Phone: (314) 286-2764 Fax: (314) 286-2784 gitlin@wustl.edu.

insulin sensitivity (Bui and Thompson, 2006; Hardie, 2007; Semenza, 2007). Decreasing oxygen tensions prevent a family of prolyl hydroxylases that utilize molecular oxygen from hydroxylating and destabilizing HIF, permitting HIF-dependent expression of genes essential for hypoxic adaptation (Hirota and Semenza, 2005; Lahiri et al., 2006). AMPK is a heterotrimeric complex that is activated by increased phosphorylation following allosteric interaction with AMP and performs a central function in cellular as well as organismal energy homeostasis by regulating multiple, well characterized downstream targets (Jones et al., 2005; Mandal et al., 2005; Hardie et al., 2006; Long and Zierath, 2006). The growing understanding of these mechanisms of biochemical adaptation has yet to be integrated with the regulation of metabolism during development.

Developing organisms possess two characteristics that may permit broader mechanistic insight into metabolic adaptation at other stages of life. First, the intrinsically dynamic process of development may permit the direct comparison of anoxia tolerant, anoxia sensitive, and intermediate states in the same developing organism, making the correlation of molecular phenotypes with the precise degree of anoxia tolerance possible. Some currently used models of anoxia tolerance require comparison with different anoxia sensitive species, potentially obscuring the identification of metabolic and biochemical mechanisms fundamental to such tolerance (Suarez et al., 1989).

Second, a vertebrate model of anoxia tolerance with a sequenced genome and amenable to forward and reverse genetic analysis would assist the identification of important components of these pathways and the study of their evolutionary context. A forward genetic approach has been successfully applied in the nematode *C. elegans* to identify the role of key components of the cell cycle in anoxia tolerance in this invertebrate (Padilla et al., 2002; Nystul et al., 2003). This approach could be utilized to elucidate additional regulators of both normoxic and anoxic metabolism, though a genetically accessible vertebrate model with well-characterized bioenergetics and responses to anoxia is currently lacking. Recently, Padilla *et al*. demonstrated that zebrafish embryos (*Danio rerio*) can survive in anoxia, a phenomenon they refer to as “suspended animation,” and that the embryos transition from anoxia tolerance to sensitivity during development (Padilla and Roth, 2001). This observation highlights the potential for the zebrafish embryo to complement existing models with the advantage of being amenable to high-throughput genetic and small molecule methodologies in the laboratory setting.

In this study we now examine the bioenergetics of early zebrafish development with relation to anoxia tolerance. This work further investigates the role of energy sensing in the response of the zebrafish embryo to anoxia by assaying developmental arrest in mitochondrial inhibitors and assesses the activation of the energy-sensing AMPK pathway. Our observations provide insight into the regulation of metabolism during development and define the zebrafish embryo as a vertebrate model with the potential to add forward genetic and small molecule screens to the arsenal of experimental approaches available to the study of anoxia tolerance.

Results

Transition in Anoxia Tolerance

Among the most fascinating aspects of zebrafish anoxia tolerance is the loss of this tolerance, the timing of which has not been fully analyzed. To characterize the transition from anoxia tolerance to sensitivity in the developing zebrafish, we placed embryos at different developmental stages into anoxia for increasing durations and counted the proportion of those embryos that resumed development upon the return to normoxia. As can be seen from the results in Fig. 1A, these experiments revealed that older embryos survived

for decreasing time periods in anoxia, a finding consistent with a previous report (Padilla and Roth, 2001). When this duration of viability at each given developmental stage was examined as a function of the age of the embryo, the resulting analysis demonstrated a linear decline such that each additional hour of development resulted in the loss of one hour of viability in anoxia (Fig. 1B). Anoxic lethality occurred at approximately 52 hours post fertilization (hpf) regardless of the proportion of that time spent in normoxia or anoxia.

We next sought to determine the effect of prolonged exposure to anoxia on subsequent anoxia tolerance. We placed 24 hpf embryos into anoxia for a sub-lethal duration of 24 h, allowed them to recover in normoxia for 4 h and then returned them to an anoxic environment. Under these experimental conditions, embryos survived in anoxia beyond 52 hpf (Fig. 2A, dotted line), and the duration of viability in the second anoxic exposure was indistinguishable from that expected following a first anoxic exposure in 28 hpf embryos, the approximate developmental stage of these embryos (Fig. 2A).

Fig. 1A and Fig. 1B suggest that the developmental stage is an important factor in the duration of anoxic viability. To study the effect of processes occurring during anoxia on the duration of anoxic viability, we examined the temperature sensitivity of the anoxic zebrafish embryo by conducting anoxic survival studies at varying ambient temperatures which have been demonstrated to directly affect metabolic rate as determined by oxygen consumption in the zebrafish (Fig. S1) and in other models (Barrionuevo and Burggren, 1999; Bickler and Buck, 2007). The duration of viability in anoxia was inversely correlated with the temperature during the period of anoxic exposure (Fig. 2B).

Metabolic Suppression During Anoxia

Defining an index of metabolic suppression that accompanies the switch from aerobic to anaerobic energy production is vital to understanding the adaptation of the zebrafish to anoxia and for establishing this organism as an anoxia tolerant model system (Guppy and Withers, 1999). To this end we measured the rates of oxygen consumption in normoxia and lactate accumulation in anoxia. These experiments revealed that the rate of oxygen consumption in the zebrafish embryo increased approximately linearly with developmental time in normoxia over the first two days of development, with each developmental stage using oxygen at a characteristic rate (Fig. 3A). Similarly, anoxic embryos accumulated lactate at a rate characteristic of the developmental stage at which they were placed into anoxia. However, the change in the rate of lactate accumulation in anoxia across stages was not linear but rather increased slowly and then accelerated (Fig. 3B).

Using normoxic oxygen consumption and anoxic lactate accumulation to determine ATP production, we calculated the percentage of normoxic ATP production that occurred in anoxia as an index of metabolic suppression. The relative metabolic rate in anoxia compared to normoxia describes a U-shaped curve over the first 48 h of development (Fig. 3C). For the first 24 hpf, the rate of ATP production in anoxia represented a decreasing proportion of normoxic ATP production, suggesting an increased relative metabolic suppression. Then, after 24 hpf, this ratio began to increase. To determine if the duration of anoxic viability correlated with any of these metabolic parameters, we compared the decreasing anoxic viability (Fig. 1B) with the rate of oxygen consumption, lactate accumulation, and calculated metabolic suppression. The duration of anoxic viability at each stage correlated inversely with the rate of anoxic lactate accumulation at that same stage (Fig. 3D).

Proximate Signal for Developmental Arrest

Early embryologic studies in another teleost model have demonstrated that reversible developmental arrest can occur in normoxia in the presence of cyanide, an inhibitor of

cytochrome *c* oxidase, or dinitrophenol, a protonophore that uncouples respiration from ATP synthesis (Crawford and Wilde, 1966). To determine if interference in these processes or additional components of mitochondrial oxidative phosphorylation was sufficient to cause an arrest similar to that observed in anoxia in the zebrafish embryo we incubated normoxic embryos in potassium cyanide (KCN), carbonyl cyanide *m*-chlorophenylhydrazone (CCCP), a protonophore, rotenone, which inhibits complex I, myxothiazole, which inhibits complex III, and oligomycin and dicyclohexylcarbodiimide (DCCD), two inhibitors of the ATP synthase (Fig. 4A) (Wyatt and Buckler, 2004). All of these drugs recapitulated the arrest observed in anoxia (Fig. 4B,C), with two important exceptions. First, rotenone, myxothiazole, oligomycin and DCCD are known to be irreversible inhibitors and thus embryos remained arrested upon washing of these drugs (Moreno-Sanchez et al., 1999; von Ballmoos et al., 2004; Wyatt and Buckler, 2004). KCN and CCCP were reversible (Fig. 4B,C), and embryos arrested in both recovered (Fig. 4C) and could be grown to adulthood (data not shown). Second, treatment of embryos with any of these small molecules consistently resulted in a more rapid arrest and shorter duration of viability than that observed in anoxia (data not shown). The duration of viability was consistent with the difference in the rate of lactate accumulation between anoxia and these small molecules (Fig. 4D). Furthermore, we observed that the rate of lactate accumulation was similar between the reversible and irreversible inhibitors (Fig. 4D) and did not vary if embryos remained in an irreversible inhibitor or if it was washed off (Fig. 4E) demonstrating that normoxic embryos in irreversible inhibitors were metabolizing anaerobically and were therefore alive.

As complete arrest can be mediated by a decline in oxidative phosphorylation independent of oxygen status, we hypothesized that impairment of oxidative phosphorylation might underlie intermediate rates of growth observed in hypoxia (Kajimura et al., 2005). To examine this, we incubated embryos in a range of KCN concentrations and observed their rate of development. Increasing KCN concentrations caused a continuous exponential decline in the developmental rate until growth was arrested altogether (Fig. 4F).

AMPK Pathway Activation during Developmental Arrest

To our knowledge the role of AMPK has not been studied in the context of anoxia tolerance, and we reasoned that activation of this kinase following anoxic perturbation of ATP synthesis could play a central role in metabolic arrest in anoxia tolerant organisms by linking energy sensing to the reduction of metabolic demand. Consistent with this concept, both anoxia and KCN treatment of normoxic embryos at 24 hpf resulted in the rapid phosphorylation of AMPKα (Fig. 5A) as well as the direct AMPK target Acetyl-CoA Carboxylase (ACC), a key enzyme in fatty acid synthesis (Fig. 5B) (Long and Zierath, 2006). Furthermore, both anoxia and KCN treatment resulted in the rapid inactivation by dephosphorylation of p70-S6-Kinase (S6K), a kinase essential for protein synthesis downstream of the target of rapamycin (TOR), a central signaling protein that coordinates cell growth with the cellular energy state (Fig. 5C) (Inoki et al., 2003;Schieke and Finkel, 2007). In older embryos the activation of the AMPK pathway became extremely rapid, with abundant phosphorylation appearing after 1 min in KCN in 72 hpf embryos (Fig. 5D). Consistent with these findings, incubation of 24 hpf embryos in KCN for 5 min resulted in a dramatic increase in the AMP/ATP ratio (Fig. 5E) suggesting that AMPK is activated via the increase in the AMP/ATP ratio. Total ATP levels also declined in KCN and more slowly in anoxia (data not shown), consistent with the slower rate of arrest observed in anoxia.

Discussion

Implications of a Reversible Arrest

The findings in this study reveal that the duration of anoxic viability in the zebrafish embryo declines gradually with the developmental stage and anaerobic metabolic rate (Figs. 1-3), that the inhibition of oxidative phosphorylation is sufficient to cause a developmental arrest (Fig. 4), and that conditions that cause arrest activate the AMPK pathway (Fig. 5). A simple conclusion to be drawn from the phenomenon of a reversible arrest, though to our knowledge not previously articulated, is that no information can be encoded in the inertia of the developmental program. The tempo of morphogen diffusion or differentiation in response to the segmentation clock, for example, cannot depend on the intrinsic pace of these processes as they can be completely halted and restarted. The robust recovery of arrested embryos requires either a “place holder” mechanism or a system to reestablish the timing of development. Such processes, likely fundamental to normoxic development as well, may be experimentally accessible using this model of arrest and recovery.

Zebrafish as a Model of Recovery from Arrest

Zebrafish embryos allowed to briefly recover from anoxia rapidly regained the expected duration of anoxic viability for their developmental stage (Fig. 2A). These findings argue against a model in which the duration of anoxic viability is determined by a decreasing energy store such as glycogen as this recovery would require the resynthesis of glycogen without any caloric intake. Instead, normoxic recovery may permit the reestablishment of energy homeostasis, in effect “resetting” the embryo, or may involve a process of preconditioning in which the anoxic insult prepares the organism for a subsequent bout (Iliodromitis et al., 2007). Adaptations necessary for recovery such as the antioxidant response to reoxygenation and the mechanisms underlying preconditioning are incompletely understood. Both may be experimentally accessible in the zebrafish model.

Energy is the Proximate Signal for Developmental Arrest

We reasoned it unlikely that anoxic arrest evolved in response to chemical inhibitors of oxidative phosphorylation, suggesting that the small molecules used in these studies function by mimicking a critical signal initiated by anoxia. Because oxygen is available in the presence of these chemical inhibitors, the observation of a reversible arrest implies that developmental arrest is not entirely induced by the sensing of molecular oxygen independent of its role in cellular respiration. The concept that oxygen is sensed by its role in mitochondrial function is not novel (Wyatt and Buckler, 2004), though it is controversial in part due to important observations such as the physiologic responses of oxygen conforming systems to reduced oxygen tensions at levels that do not limit respiration (Boutilier and St-Pierre, 2000; Hochachka and Somero, 2002). Nevertheless, mitochondria are uniquely situated to function as oxygen sensors and have been studied in this context (Buck and Pamenter, 2006). Detailed experiments performed in carotid body type I cells have shown mitochondrial ATP metabolism to be central to the detection of hypoxia (Wyatt and Buckler, 2004). The small molecules utilized in this study exert unique and opposing effects on respiration, mitochondrial membrane potential, and the activity of specific respiratory complexes, though all prevent ATP synthesis by oxidative phosphorylation. As these small molecules and anoxia produced similar phenotypes, our findings indicate that the inhibition of the ATP synthesis activity of oxidative phosphorylation is a relevant common signal and is sufficient to cause arrest.

We have also noted that arrest following chemical mitochondrial inhibition is associated with a shorter duration of viability and greater lactate production than observed in anoxia (Fig. 4D). Due to these differences, the survival studies in chemical inhibitors were

performed at 24° C rather than 28.5° C to confirm a duration of viable arrest of at least 24 h (Fig. 4B,C). Several models may account for these differences. A portion of the metabolic suppression observed in anoxia could require a molecular oxygen sensor independent of oxidative phosphorylation. Alternatively, intrinsic experimental differences could account for this reduced duration of viability. The chemical inhibitors caused a much more rapid arrest than anoxia and may have more completely inhibited oxidative phosphorylation than an anoxic environment would if it contained trace oxygen. Regardless, diverse means of inhibiting oxidative phosphorylation induced a substantial metabolic suppression and caused a viable developmental arrest, suggesting an important role for energy sensing in anoxia tolerance.

Further support for the concept that mitochondrial energy production acts as a critical oxygen sensor may be obtained by genetic methodologies interfering with oxidative phosphorylation. However, this approach is complicated by the presence of abundant maternal mitochondria and a dearth of available strains with mutations affecting electron transport chain complexes. Antisense morpholino oligonucleotide knockdown of mitochondrial components has been employed, though this method did not reduce the activity of the targeted complexes to less than half of normal, likely explaining why these experiments did not produce an arrest phenotype (Baden et al., 2007). Nevertheless, dominant negative or temperature sensitive alleles of electron transport chain subunits would permit the highly specific control of mitochondrial energy production and may allow more detailed studies of the cell autonomy of arrest or the effects of mitochondrial inhibition on specific tissues or cell types. Furthermore, a forward genetic approach would offer an opportunity to identify mutations that alter or mimic the response to anoxia.

Energy Status Regulates Developmental Rate

Slowed growth in hypoxia has been observed in the zebrafish and hypothesized to result from HIF-mediated perturbation of insulin-like growth factor signaling (Kajimura et al., 2005). However, the immediacy of arrest observed utilizing chemical inhibitors argues against a process involving HIF-dependent new gene expression. Consistent with this concept, no interruption of anoxic survival was observed under circumstances where HIF1α expression was reduced (Fig. S2) and arrest of normal development was not observed with HIF agonists such as cobalt chloride and desferroxamine (data not shown) nor in genetic mutants with upregulated HIF expression (personal communication, Dr. Rachel Giles). Reactive oxygen species have also been shown to mediate HIF stabilization (Guzy et al., 2005), though such a signal is unlikely in these studies given the different mechanisms of action of each inhibitor. Thus our studies with intermediate doses of KCN indicate that the rate of oxidative phosphorylation is an important effector of hypoxic growth retardation (Fig. 4F) and must therefore lie upstream of any role for HIF-mediated growth factor perturbation.

AMPK in Energy Homeostasis During Development

Despite elucidation of many of the physiologic principles of anoxic adaptation, the processes that link reductions in metabolic rate to reductions in energy consumption remain elusive (Bickler and Buck, 2007). AMPK regulates translation, one of the most energy-expensive cellular processes (Hochachka et al., 1996; Inoki et al., 2003; Jones et al., 2005), by signaling through the tuberous sclerosis complex to the TOR pathway, and also stimulates glycolysis, suppresses fatty acid synthesis, influences the cell cycle through the action of p53 (Mandal et al., 2005; Thoreen and Sabatini, 2005) and alters cell structure via the myosin regulatory light chain (Hardie et al., 2006; Lee et al., 2007). Given these central roles in metabolism and the findings noted above, we reasoned that the oxygen-independent energy sensing AMPK pathway may function to link energy supply and demand during the

anoxic response. Interestingly, as these studies of the AMP/ATP ratio and AMPK activation involve whole embryos (Fig. 5) it is possible that such changes vary by tissue type, though if these changes only occur in restricted tissues they must be even larger than reported here. Importantly, the slower kinetics of AMPK activation following anoxia (Fig. 5A-C) compared to KCN reflected the delay in time to arrest under anoxia as discussed above, demonstrating that phosphorylation of AMPK and its targets correlates directly with the timing of onset of suspended animation. Notably, in the carotid body model discussed above, the observed excitation caused by the same stimuli that arrest zebrafish embryos has been demonstrated to be mediated by AMPK (Wyatt et al., 2007). Thus AMPK may serve as a regulatory nexus for anoxic adaptation.

Neither antisense morpholino oligonucleotides, dominant-negative constructs nor chemical inhibitors sufficiently reduced AMPK activity in the zebrafish embryo to determine the necessity of this kinase in anoxic survival, in part due to the presence of abundant maternally-derived AMPK protein (Fig. S3). Consistent with this idea, embryonic loss of AMPK activity required generation of a maternal/zygotic mutant in *Drosophila* (Lee et al., 2007) and therefore our current studies are focused on this approach in zebrafish to directly examine the role of AMPK in anoxia tolerance.

Developmental Acquisition of Anoxia Sensitivity

Our observations that the developmental rate (Fig. 4F) and the duration of anoxic viability (Fig. 1) vary continuously without abrupt transitions would not have been possible by comparing anoxia tolerant and sensitive species. An understanding of the processes underlying this gradual acquisition of anoxia sensitivity would be of tremendous benefit in relation to the hypoxic injury of anoxia sensitive human tissues. The gradual decrease in the duration of anoxic viability correlates with the rate of anoxic lactate accumulation (Fig. 3D), which could imply a model in which the machinery for metabolic suppression disappears, though the ability to control metabolism would be adaptive at all developmental stages and would likely be maintained throughout the life of the organism. Indeed, AMPK was activated after as little as 1 min of KCN treatment in 72 hpf embryos (Fig. 5D), though embryos at this stage survive less than 10 min in KCN.

We favor a model in which new energy-requiring processes in development differ in the degree to which they must be supported by anaerobic fermentation in anoxia. An embryo that disproportionately increased its normoxic metabolism in earlier stages with processes that do not require energy in anoxia would extend the developmental window in which it was anoxia tolerant. This model would explain how an embryo with a linearly increasing normoxic metabolic rate (Fig. 3A) could achieve the observed non-linear increase in anaerobic metabolism with age (Fig. 3B) and thus a U-shaped pattern of metabolic suppression (Fig. 3C). A zebrafish embryo covered by brood-mates could experience anoxia and it is intriguing to note that this anoxia tolerant window appears to close at approximately 52 hpf, the time when its siblings would begin to hatch and swim away. The perspective that anoxia tolerance may also differ only as a matter of degree among different species offers insight into the apparent independent evolution of anoxia tolerance in diverse species (Hochachka and Lutz, 2001).

The Zebrafish Embryo as a Model of Anoxia Tolerance

In addition to providing insight into the metabolic coordination of development, the zebrafish embryo complements existing models by providing a platform for genetic and small molecule screens to permit mechanistic insight into processes of energy sensing, oxygen sensing and metabolic suppression. Importantly, the imbalances in cellular ATP levels experienced by anoxic zebrafish embryos (Fig. 5E) resemble the metabolic

perturbations in anoxia sensitive human tissue more closely than do models that maintain energy balance in anoxia. Understanding why such metabolic perturbations are tolerated by the zebrafish might suggest interventions for human ischemic disease. Indeed, for such approaches the zebrafish is an elegant example of the Krogh principle, perhaps defining an ideal species in which to study the mechanisms of anoxia tolerance during development (Somero, 2000).

Experimental Procedures

Materials and Environmental Conditions

All chemical reagents were purchased from Sigma-Aldrich (St. Louis, MO) unless noted otherwise. Morpholino oligonucleotides were purchased from GeneTools (Corvalis, OR). Normoxia is defined as room air consisting of an approximate 78:20 ratio of nitrogen and oxygen, water vapor and trace carbon dioxide. An anoxic environment was created with a Bactron II anaerobic chamber (Shel Labs, Cornelius, OR), which contains an atmosphere of 90% N_2, 5% CO_2, and 5% H_2 and a temperature-controlled incubator. A palladium catalyst, which removes residual oxygen by reaction with H_2, was reactivated by heating to above 160° C and replaced daily. To account for potential acidification of egg water by CO_2, all egg water was buffered with 1 mg/mL sodium bicarbonate, pH 7.1. No developmental abnormalities were observed in this egg water, the stability of the pH of this egg water was verified in normoxia and anoxia, and it was used in both normoxic and anoxic experiments. Incubation of embryos in 5% CO_2 plus room air in buffered egg water did not alter the rate or morphology of development nor the effect of the chemical inhibitors on arrest.

Experimental Animals

Wild type zebrafish (AB strain) were maintained in a 14h-light/10h- dark cycle and housed according to guidelines approved by the Washington University Animal Studies Committee. Embryos were obtained by *in vitro* fertilization to maximize developmental synchronization. Embryos were raised at 28.5° C unless otherwise stated and staged according to Kimmel *et al*. (Kimmel et al., 1995). Images were taken with an SZX12 zoom stereomicroscope (Olympus).

Anoxic viability experiments

Embryonic stage is defined as hours post fertilization at 28.5° C as described by Kimmel et al. (Kimmel et al., 1995). Embryos at each stage were placed into anoxia in 2 mL of egg water in 6-well plates, 20 embryos per well, and were incubated at 28.5° C. At intervals, plates were removed, normoxic water was added, dead embryos were removed, and the embryos were allowed to recover for 24 h, at which point the viability at that stage and duration of anoxia was assessed. Death was defined as having partially or completely disintegrated, and recovery was defined as developmental progression. Each point reflects 2 wells of 20 embryos each, repeated twice independently and averaged. Temperature sensitivity was determined by incubating 24 hpf embryos at the indicated temperature as described above. Each point represents 4 wells of 20 embryos, repeated twice.

Respirometry

Oxygen consumption was measured with the OX1LP 4 mL respirometer (Qubit Systems, Kingston, ON), which uses a Clark-type electrode. After equilibration and heating to 28.5° C and calibration per the manufacturer's protocol, the background oxygen consumption by the sensor in 3 mL of egg water was measured, which was subtracted from the rate observed including embryos. Each point represents 2-4 separate measurements at the stage indicated and averaged. Points at 4 hpf and 10 hpf represent single measurements. Because the

majority of embryonic mass is non-metabolic yolk, measurements of oxygen consumption are expressed per embryo rather than per unit mass because.

Lactate and nucleotide assays

Embryos were incubated in anoxia at 28.5° C beginning at the indicated developmental stage. The rate of lactate accumulation was calculated by the best-fit line to multiple points of increasing duration in anoxia, each consisting of 2 samples of 10 embryos. Embryos were thoroughly homogenized in 80 μl 1.2 M perchloric acid, centrifuged to remove insoluble material, and the resulting supernatant was added to 1 ml of a 1:3 diluted glycine buffer (Sigma-Aldrich #G5418) with 1.67 mg/mL NAD+ and 16.7 U/mL lactate dehydrogenase. The samples were gently mixed and allowed to react for 1 h at room temperature, after which end-point NADH production was detected by absorption at 340 nm in a Lambda 45 spectrophotometer (Perkin-Elmer, Waltham, MA). Absolute quantities of lactate were calculated by comparison to a standard curve. Rates are expressed per embryo as discussed above. The AMP/ATP ratio was determined by HPLC analysis using 5 embryos per sample, three samples per condition, as described previously (Dasgupta and Milbrandt, 2007). Total ATP was measured by the ENLITEN luciferase ATP assay kit using manufacturer-supplied instructions (Promega, Madison, WI).

Calculation of Index of Metabolic Suppression

To calculate the percentage of normoxic ATP production that occurs in anoxia, we assumed that non-mitochondrial oxygen consumption was negligible or was at least a constant proportion of total oxygen use throughout development. We have observed lactate accumulation in normoxic zebrafish embryos to be negligible (data not shown). Finally, we have assumed that the P/O ratio (moles of ATP produced per mole of atomic oxygen consumed) equals 2.8 (Boutilier, 2001), and remains constant during the time period analyzed here. The index of metabolic suppression was calculated by dividing the rate of ATP production in anoxia as determined by lactate accumulation by the rate of ATP production in normoxia as determined by oxygen consumption at each developmental stage indicated.

Drug treatments

Potassium cyanide (KCN, 1 M stock solution in water) was used at 1 mM unless stated otherwise. Cyanide is volatile and was used in sealed tubes in parallel with untreated embryos in sealed tubes to ensure that oxygen did not become limiting. Carbonyl cyanide *m*-chlorophenylhydrazone (CCCP, 100 mM stock solution in DMSO) was used at 100 μM in buffered egg water containing 1 mg/mL sodium bicarbonate at pH 7.1. Survival in the other drugs was similar in buffered and unbuffered egg water. Rotenone (20 mM stock solution in DMSO) was used at 1 μM. Myxothiazole (20 mM stock solution in methanol) was used at 500 nM. Oligomycin (10 mM stock solution in ethanol) was used at 10 μM and washed after 1.5 h of treatment. Dicyclohexylcarbodiimide, (DCCD, purchased as a 1 M stock solution in dichloromethane) was used at 100 μM and was washed after 1 h of treatment. For the drug survival studies, the number of embryos used was as follows: anoxia: n=120 embryos, cyanide: n=310, rotenone: n=150, CCCP: n=240, myxothiazole: n=210, oligomycin: n=150, and DCCD: n=100. The numbers reported are from two separate experiments, each consisting of 2-4 separate plates of each drug. All experiments comparing the viability and recovery in these drugs were performed at 24° C. For determination of developmental rate in cyanide, embryos were placed in a range of doses of KCN or in no drug in sealed tubes at 5 embryos per tube. After 24 h the embryos were examined and assigned a numerical age according to their developmental stage as defined by Kimmel *et al*. (Kimmel et al., 1995). These were compared to the untreated embryos and growth rate was calculated as: (hours

aged in KCN)/(hours aged in the control). Data consists of the averages of 2 separate experiments, each with 2 tubes per dose.

Immunoblot Studies

10 embryos/sample were incubated at 24° C in the indicated dose of KCN or at 28.5° C in anoxia for the indicated durations. Embryos were lysed in RIPA buffer containing 25 μl/ml protease inhibitor cocktail (Calbiochem, San Diego, CA) and 150 μl/ml phosphatase inhibitor cocktail (Calbiochem), dounced, centrifuged to remove insoluble material, and subjected to SDS-PAGE. All primary antibodies were used at 1:1000 dilution. The antibodies used were #3661 (Phospho-Acetyl-CoA Carboxylase, Ser79), #3662 (Acetyl-CoA Carboxylase, total) #2531 (Phospho-AMPKα, Thr172), #2532 (AMPKα, total), #9234 (Phospho-p70 S6 Kinase, Thr389), #9202 (p70 S6 Kinase, total), all from Cell Signaling Technology (Danvers, MA). Sequence alignments between the human proteins to which these antibodies were produced and the homologous zebrafish sequences revealed the conservation of these phosphorylated residues as well as the surrounding sequence, though the phosphorylated residues in the zebrafish proteins do not occur at exactly the same amino acid number. Blots were probed with 1:10,000 HRP-conjugated goat anti-rabbit secondary antibody (Pierce, Rockford, IL) and developed using the SuperSignal West Femto Maximum Sensitivity Substrate (Pierce).

Supplementary Material

Refer to Web version on PubMed Central for supplementary material.

Acknowledgments

Amy Koerber provided expert zebrafish husbandry. We thank Stephen Johnson, Lou Muglia and Josh Rubin for careful review of the manuscript. This work was supported by National Institutes of Health grants DK44464 and DK61763 (J.D.G.), Medical Scientist Training Program Grant T32 GM07200 (B.A.M.) and the Chancellor's Hartwell Prize for Innovative Research from Washington University (J.D.G.).

References

Baden KN, Murray J, Capaldi RA, Guillemin K. Early developmental pathology due to cytochrome c oxidase deficiency is revealed by a new zebrafish model. J Biol Chem. 2007; 282:34839–34849. [PubMed: 17761683]

Barrionuevo WR, Burggren WW. O2 consumption and heart rate in developing zebrafish (Danio rerio): influence of temperature and ambient O2. Am J Physiol. 1999; 276:R505–513. [PubMed: 9950931]

Bickler PE, Buck LT. Hypoxia tolerance in reptiles, amphibians, and fishes: life with variable oxygen availability. Annu Rev Physiol. 2007; 69:145–170. [PubMed: 17037980]

Boutilier RG. Mechanisms of metabolic defense against hypoxia in hibernating frogs. Respir Physiol. 2001; 128:365–377. [PubMed: 11718764]

Boutilier RG, St-Pierre J. Surviving hypoxia without really dying. Comp Biochem Physiol A Mol Integr Physiol. 2000; 126:481–490. [PubMed: 10989340]

Buck LT, Pamenter ME. Adaptive responses of vertebrate neurons to anoxia--matching supply to demand. Respir Physiol Neurobiol. 2006; 154:226–240. [PubMed: 16621734]

Bui T, Thompson CB. Cancer's sweet tooth. Cancer Cell. 2006; 9:419–420. [PubMed: 16766260]

Crawford RB, Wilde CE Jr. Cellular differentiation in the anamniota. II. Oxygen dependency and energetics requirements during early development of teleosts and urodeles. Exp Cell Res. 1966; 44:453–470. [PubMed: 5964765]

Dasgupta B, Milbrandt J. Resveratrol stimulates AMP kinase activity in neurons. Proc Natl Acad Sci U S A. 2007; 104:7217–7222. [PubMed: 17438283]

Guppy M, Withers P. Metabolic depression in animals: physiological perspectives and biochemical generalizations. Biol Rev Camb Philos Soc. 1999; 74:1–40. [PubMed: 10396183]

Guzy RD, Hoyos B, Robin E, Chen H, Liu L, Mansfield KD, Simon MC, Hammerling U, Schumacker PT. Mitochondrial complex III is required for hypoxia-induced ROS production and cellular oxygen sensing. Cell Metab. 2005; 1:401–408. [PubMed: 16054089]

Hardie DG. AMP-activated/SNF1 protein kinases: conserved guardians of cellular energy. Nat Rev Mol Cell Biol. 2007

Hardie DG, Hawley SA, Scott JW. AMP-activated protein kinase--development of the energy sensor concept. J Physiol. 2006; 574:7–15. [PubMed: 16644800]

Hirota K, Semenza GL. Regulation of hypoxia-inducible factor 1 by prolyl and asparaginyl hydroxylases. Biochem Biophys Res Commun. 2005; 338:610–616. [PubMed: 16154531]

Hochachka PW, Buck LT, Doll CJ, Land SC. Unifying theory of hypoxia tolerance: molecular/metabolic defense and rescue mechanisms for surviving oxygen lack. Proc Natl Acad Sci U S A. 1996; 93:9493–9498. [PubMed: 8790358]

Hochachka PW, Lutz PL. Mechanism, origin, and evolution of anoxia tolerance in animals. Comp Biochem Physiol B Biochem Mol Biol. 2001; 130:435–459. [PubMed: 11691622]

Hochachka, PW.; Somero, GN. Biochemical adaptation : mechanism and process in physiological evolution. Oxford University Press.; Oxford ; New York: 2002. p. xip. 466

Iliodromitis EK, Lazou A, Kremastinos DT. Ischemic preconditioning: protection against myocardial necrosis and apoptosis. Vasc Health Risk Manag. 2007; 3:629–637. [PubMed: 18078014]

Inoki K, Zhu T, Guan KL. TSC2 mediates cellular energy response to control cell growth and survival. Cell. 2003; 115:577–590. [PubMed: 14651849]

Jones RG, Plas DR, Kubek S, Buzzai M, Mu J, Xu Y, Birnbaum MJ, Thompson CB. AMP-activated protein kinase induces a p53-dependent metabolic checkpoint. Mol Cell. 2005; 18:283–293. [PubMed: 15866171]

Kajimura S, Aida K, Duan C. Insulin-like growth factor-binding protein-1 (IGFBP-1) mediates hypoxia-induced embryonic growth and developmental retardation. Proc Natl Acad Sci U S A. 2005; 102:1240–1245. [PubMed: 15644436]

Kemp PJ. Detecting acute changes in oxygen: will the real sensor please stand up? Exp Physiol. 2006; 91:829–834. [PubMed: 16857717]

Kimmel CB, Ballard WW, Kimmel SR, Ullmann B, Schilling TF. Stages of embryonic development of the zebrafish. Dev Dyn. 1995; 203:253–310. [PubMed: 8589427]

Lahiri S, Roy A, Baby SM, Hoshi T, Semenza GL, Prabhakar NR. Oxygen sensing in the body. Prog Biophys Mol Biol. 2006; 91:249–286. [PubMed: 16137743]

Lee JH, Koh H, Kim M, Kim Y, Lee SY, Karess RE, Lee SH, Shong M, Kim JM, Kim J, Chung J. Energy-dependent regulation of cell structure by AMP-activated protein kinase. Nature. 2007; 447:1017–1020. [PubMed: 17486097]

Long YC, Zierath JR. AMP-activated protein kinase signaling in metabolic regulation. J Clin Invest. 2006; 116:1776–1783. [PubMed: 16823475]

Mandal S, Guptan P, Owusu-Ansah E, Banerjee U. Mitochondrial regulation of cell cycle progression during development as revealed by the tenured mutation in Drosophila. Dev Cell. 2005; 9:843–854. [PubMed: 16326395]

Moreno-Sanchez R, Bravo C, Westerhoff HV. Determining and understanding the control of flux. An illustration in submitochondrial particles of how to validate schemes of metabolic control. Eur J Biochem. 1999; 264:427–433. [PubMed: 10491087]

Nystul TG, Goldmark JP, Padilla PA, Roth MB. Suspended animation in C. elegans requires the spindle checkpoint. Science. 2003; 302:1038–1041. [PubMed: 14605367]

Padilla PA, Nystul TG, Zager RA, Johnson AC, Roth MB. Dephosphorylation of cell cycle-regulated proteins correlates with anoxia-induced suspended animation in Caenorhabditis elegans. Mol Biol Cell. 2002; 13:1473–1483. [PubMed: 12006646]

Padilla PA, Roth MB. Oxygen deprivation causes suspended animation in the zebrafish embryo. Proc Natl Acad Sci U S A. 2001; 98:7331–7335. [PubMed: 11404478]

Podrabsky JE, Lopez JP, Fan TW, Higashi R, Somero GN. Extreme anoxia tolerance in embryos of the annual killifish Austrofundulus limnaeus: insights from a metabolomics analysis. J Exp Biol. 2007; 210:2253–2266. [PubMed: 17575031]

Schieke SM, Finkel T. TOR and aging: less is more. Cell Metab. 2007; 5:233–235. [PubMed: 17403368]

Semenza GL. Life with oxygen. Science. 2007; 318:62–64. [PubMed: 17916722]

Somero GN. Unity in diversity: a perspective on the methods, contributions, and future of comparative physiology. Annu Rev Physiol. 2000; 62:927–937. [PubMed: 10845117]

Suarez RK, Doll CJ, Buie AE, West TG, Funk GD, Hochachka PW. Turtles and rats: a biochemical comparison of anoxia-tolerant and anoxia-sensitive brains. Am J Physiol. 1989; 257:R1083–1088. [PubMed: 2556054]

Thoreen CC, Sabatini DM. AMPK and p53 help cells through lean times. Cell Metab. 2005; 1:287–288. [PubMed: 16054073]

von Ballmoos C, Brunner J, Dimroth P. The ion channel of F-ATP synthase is the target of toxic organotin compounds. Proc Natl Acad Sci U S A. 2004; 101:11239–11244. [PubMed: 15277681]

Wyatt CN, Buckler KJ. The effect of mitochondrial inhibitors on membrane currents in isolated neonatal rat carotid body type I cells. J Physiol. 2004; 556:175–191. [PubMed: 14724184]

Wyatt CN, Mustard KJ, Pearson SA, Dallas ML, Atkinson L, Kumar P, Peers C, Hardie DG, Evans AM. AMP-activated protein kinase mediates carotid body excitation by hypoxia. J Biol Chem. 2007; 282:8092–8098. [PubMed: 17179156]

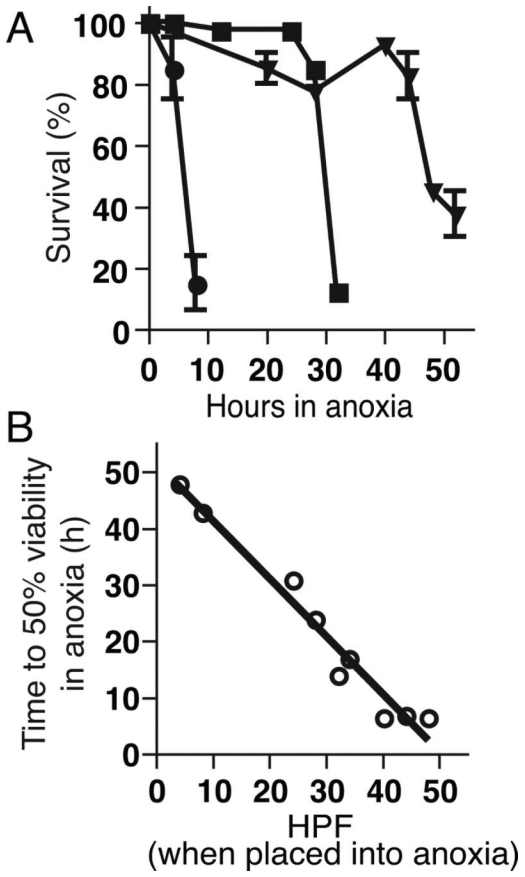

Fig. 1.

The duration of anoxic viability decreases with developmental stage. **A:** Embryos were placed into anoxia at 4 hpf (triangles), 24 hpf (squares) or 48 hpf (circles) at 28.5° C, returned to normoxia at intervals, and the percentage that had resumed development 24 h later was determined. Error bars are ±SEM. **B:** The duration of anoxia after which half of the embryos were no longer viable when returned to normoxia (open circles) plotted versus the developmental age at which the embryos were placed into anoxia, with best-fit line (slope = -1.02, $R^2 = 0.96$).

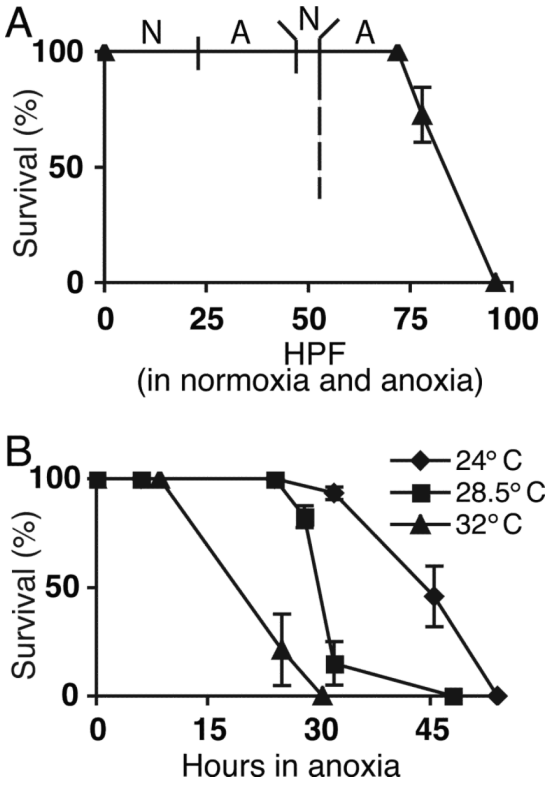

Fig. 2.

Duration of anoxic viability can be reset and varies with temperature. **A:** Embryos were allowed to develop to 24 hpf in normoxia (N) and were then placed into anoxia (A) for 24 h, removed to normoxia for 4 h, and finally returned to anoxia. The viability at time points of this second anoxic exposure was assessed (closed triangles). The dashed line indicates the 52 hpf threshold of anoxic viability observed for a first anoxic exposure at which time the embryos had only completed 28 h of normoxic development. **B:** Embryos were placed into anoxia at 24 hpf at three different temperatures, returned to normoxia at intervals, and the percentage recovering after 24 more hours was determined. Error bars are ±SD.

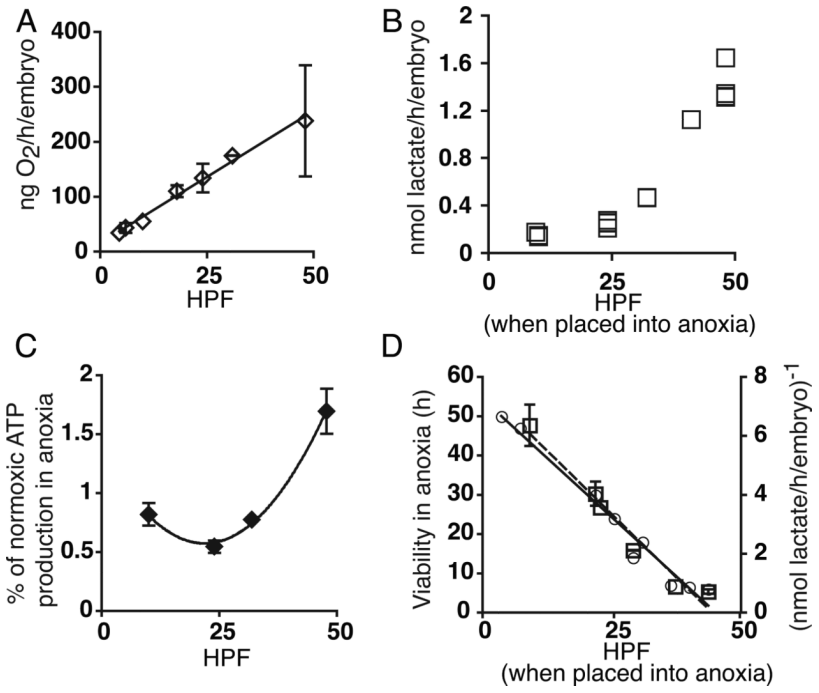

Fig. 3.

Bioenergetics and metabolic suppression in anoxia over the first two days of development. **A:** Basal oxygen consumption (open diamonds) measured at different developmental stages. **B:** The rate of lactate accumulation in anoxia per embryo (open squares). Sequential measurements of total lactate in embryos after increasing durations in anoxia were obtained and the slope of the resulting line represents the rate of lactate accumulation. This analysis was performed at different developmental stages. Each point represents the slope from one experiment. **C:** Change over developmental time in the percentage of ATP production from oxygen consumption that occurs in anoxia by lactate production, calculated as described in *Experimental Procedures*. **D:** The inverse of the rate of lactate accumulation (open squares) and best-fit line (dashed line, $R^2 = 0.96$) correlates with the duration of viability in anoxia (open circles) and best-fit line (solid line, $R^2 = 0.96$). All experiments were performed at 28.5° C. All error bars are ±SD.

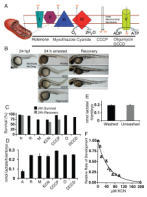

Fig. 4.

Anoxic arrest is mimicked by chemical inhibition of oxidative phosphorylation. **A:** Schematic of the electron transport chain indicating the sites of action of mitochondrial inhibitors. **B:** Images comparing embryos incubated in anoxia or various inhibitors for 24 h, and then the same embryos after 24-48 h of recovery after a return to normoxia or washing of the chemical inhibitor. **C:** The percent survival after 24 h of anoxia or treatment with chemical inhibitors beginning at 24 hpf and the percent recovery after an additional 24 h was measured. A, anoxia; R, rotenone; M, myxothiazole; O, oligomycin. **D:** Rate of lactate accumulation in 24 hpf embryos after 8 h in different mitochondrial inhibitors or anoxia. **E:** 4 hpf embryos were incubated for 1 h in 10 μM oligomycin, were washed or left in the drug for 17 additional hours, and the rate of lactate accumulation was determined. **F:** Embryos at 5 hpf placed into varying doses of KCN were incubated for 24 h after which the relative rate of growth was determined as described in *Experimental Procedures*. The best-fit line describes an exponential decline ($R^2 = 0.99$). All experiments were performed at 24° C. All error bars are ±SD.

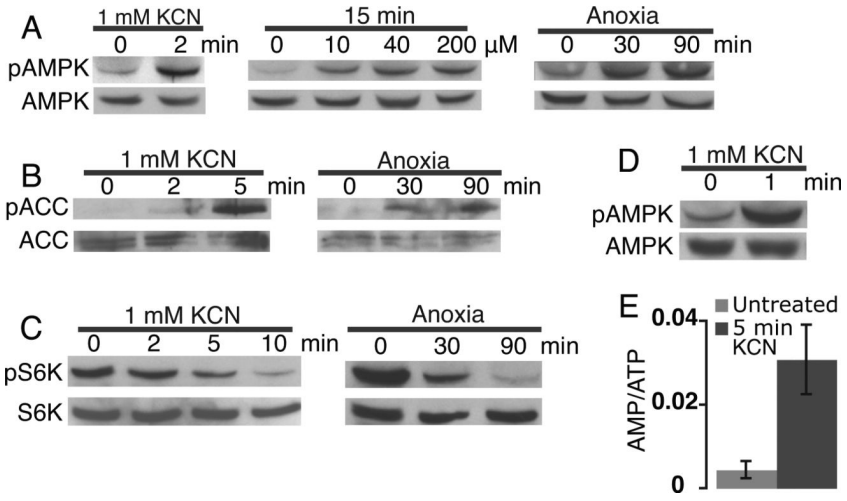

Fig. 5.

The AMP-activated protein kinase (AMPK) pathway is activated by the inhibition of oxidative phosphorylation in zebrafish embryos. **A:** Immunoblot analysis of AMPK phosphorylation before and after 2 min in KCN, with increasing KCN doses, or with increasing time in anoxia. **B:** Phosphorylation of Acetyl-CoA Carboxylase (ACC) with time in KCN or anoxia. **C:** Phosphorylation of p70-S6 Kinase (S6K) in KCN or anoxia. **D:** 72 hpf embryos were incubated in KCN and the timing of AMPK phosphorylation was assessed. **E:** Change in the AMP/ATP ratio after a 5 min inhibition of oxidative phosphorylation as described in *Experimental Procedures*. Error bars are ±SD. All experiments utilized 24 hpf embryos.